JACS
JOURNAL OF THE AMERICAN CHEMICAL SOCIETY

COMMUNICATION

pubs.acs.org/JACS

Large Spontaneous Polarization and Clear Hysteresis Loop of a Room-Temperature Hybrid Ferroelectric Based on Mixed-Halide $[BiI_3Cl_2]$ Polar Chains and Methylviologen Dication

Nicolas Leblanc,[†] Nicolas Mercier,*[,†] Leokadiya Zorina,[†,§] Sergey Simonov,[†,§] Pascale Auban-Senzier,[‡] and Claude Pasquier*[,‡]

[†]MOLTECH Anjou, UMR-CNRS 6200, Université d'Angers, 49045 Angers Cedex 01, France

[‡]Laboratoire de Physique des Solides, UMR-CNRS 8502, Bât. 510, Université Paris Sud, 91405 Orsay Cedex, France

Supporting Information

ABSTRACT: The search for hybrid organic−inorganic materials, which have the great advantage that they can be synthesized at moderate temperature ($T < 200$ °C), remains a great challenge in the field of ferroelectrics. Here, a room-temperature ferroelectric material with interesting characteristics, $(MV)[BiI_3Cl_2]$ (MV^{2+} = methylviologen), is reported. Its structure is based on polar inorganic chains resulting from a remarkable Cl/I segregation induced by methylviologen entities, which coincide with the fourfold polar axis of the tetragonal structure. Of great importance is that this room-temperature hybrid ferroelectric displays a clear electrical hysteresis loop with a large spontaneous polarization (>15 $\mu C \cdot cm^{-2}$).

Ferroelectric materials, which have numerous potential applications, are still subject to intensive research. Particularly, a great interest has been considered in the field of organic-based compounds that can be metal−organic coordination compounds (MOCCs),[1,2] ionic compounds,[3−8] or purely organic compounds.[9] These materials have the great advantage that they can be synthesized at relatively low temperature ($T < 200$ °C), at variance with inorganic compounds, which are typically synthesized at temperatures as high as 500 °C. Moreover, the hybrid materials can combine properties of the inorganic component (e.g., chemical or thermal stability) and those of the molecular organic component, which can be easily tailored. The main characteristics of ferroelectrics, which are compounds whose structure must fall in one of the 10 polar point groups, include the spontaneous polarization P_s, the shape of the hysteresis loop, and the working temperature range. In the field of hybrid ferroelectrics, however, materials with quite large room-temperature spontaneous polarizations (>1 $\mu C \cdot cm^{-2}$) and good hysteresis loops are very scarce, and the search for such materials remains a great challenge, as highlighted in recent reviews.[1a,3a] An interesting class of hybrid ferroelectrics is that of halometalate hybrids based on ns^2 metal ions of group 15 (Sb^{III} and Bi^{III}), for which the ns^2 electronic lone pair of the M^{III} center often has a key role in determining the collective properties of the material. In particular, its stereochemical activity favors the formation of acentric materials with potential optical[10] or ferroelectric properties.[4−7] Ferroelectricity has been discovered essentially in haloantimonate and halobismuthate hybrids based on the layered $M_2X_9^{3-}$ anion,[4] the 1D polymeric anions of $SbCl_4^{-}$ [5] and $Bi_2Cl_8^{2-}$,[6] and finally the $Bi_2X_{11}^{5-}$ discrete confacial bioctahedra.[7] The ferroelectric transitions and the process of polarization inversion in such hybrids are attributed to both the dynamics of the organic cation and the M^{III} ns^2 lone pair,[4−7] this last factor governing ferroelectricity in the well-known multiferroic $BiFeO_3$ inorganic compound. We recently reported on the crystal structure of the low-temperature polar phase ($T < -30$ °C) of $(MV)[BiBr_5]$ (MV^{2+}= methylviologen). However, the polarities of adjacent chains were nearly opposite to each other, with the twofold polar axis of the monoclinic system being almost perpendicular to the chains.[11] During exploration of potential ferroelectrics in this system, we discovered the compound $(MV)[BiI_3Cl_2]$ (**1**), in which polar chains resulting from the remarkable Cl/I segregation induced by methylviologen entities are parallel to the fourfold polar axis of the tetragonal structure. Of great importance is that **1** has a large room-temperature spontaneous polarization (>15 $\mu C \cdot cm^{-2}$) and displays a good electrical hysteresis loop. In this communication, we report the synthesis, single-crystal X-ray structure, and ferroelectric properties of **1**.

$(MV)[BiI_3Cl_2]$ was synthesized by the solvothermal method at 150 °C from a mixture of $BiCl_3$, 4,4′-bipyridine, and concentrated HCl and HI in methanol.[12] Dark tetragonal crystals with face sizes up to 0.4 mm × 0.4 mm were available for X-ray study and ferroelectric investigations. The structure crystallizes in the tetragonal crystal system and was refined in the space group $P4nc$,[13] which belongs to one of the 10 polar point groups, C_{4v} ($4mm$).

The structure of $(MV)[BiI_3Cl_2]$ can be described as $[BiI_3Cl_2]$ chains of trans-connected octahedra separated by methylviologen dications, defining a chessboard arrangement when viewed along the chains (Figure 1a). In the chains, two kinds of octahedra are encountered, all-iodide $Bi(2)I_6$ and mixed-halide $Bi(1)Cl_4I_2$, which alternate along the chain and are linked together via bridging iodides (Figure 1b). Both distorted octahedra are located on a fourfold axis and have four equal Bi−X bond distances in the equatorial plane [$Bi(1)-Cl_{eq}$ = 2.682(1) Å; $Bi(2)-I_{eq}$ = 3.040(1) Å] and one short [$Bi(1)-I_{bridging}(1)$ = 2.934(1) Å, $Bi(2)-I_{bridging}(2)$ = 2.973(1) Å] and one long [$Bi(1)-I_{bridging}(2)$ = 3.316(1) Å, $Bi(2)-I_{bridging}(1)$ = 3.428(2)Å] Bi−$I_{bridging}$ bond distance along the chain axis. Such a geometry corresponds well to one of the configurations described

Received: July 8, 2011
Published: August 25, 2011

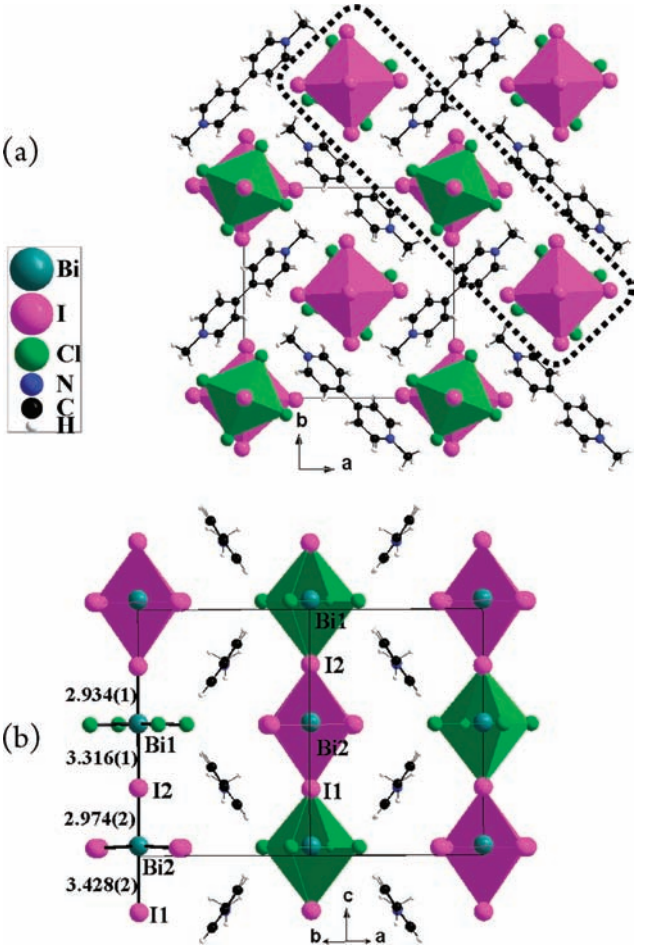

Figure 1. (a) General view of (MV)[BiI_3Cl_2] (**1**) along the polar chains. (b) View of a slice of the structure [represented inside the box in a)] showing Bi—$I_{bridging}$ bond distances in the polar chains of trans-connected BiI_6 and $BiCl_4I_2$ octahedra.

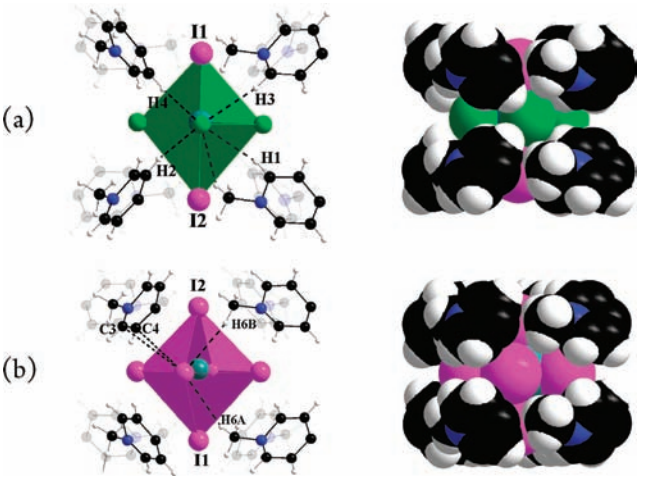

Figure 2. (left) Ball-and-stick and (right) space-filling representations of (a) $BiCl_4I_2$ and (b) BiI_6 octahedra surrounded by eight half-methylviologen entities, showing the H···Cl side contacts and pyridinium cycle···I_{eq} face contacts between the viologen entities and the equatorial chlorides ($BiCl_4I_2$ octahedra) and equatorial iodides (BiI_6 octahedra), respectively.

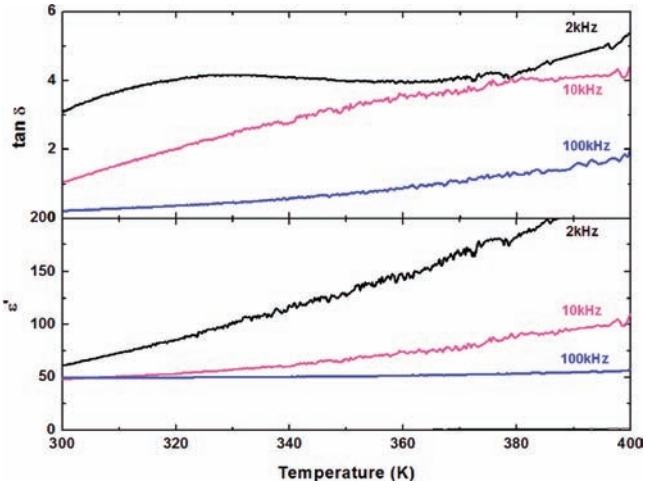

Figure 3. (top) Dielectric losses (tan δ) and (bottom) dielectric constant (ε') as functions of temperature on a single crystal of (MV)[BiI_3Cl_2]. The experiments were performed at 2, 10, and 100 kHz upon cooling at a rate of 4 K·min^{-1}.

in Brown's model,[14] indicating that the lone-pair orbital extends along the direction opposite to the short Bi—I bond and revealing the electronic $6s^2$ lone-pair stereoactivity of Bi^{3+} centers. The alternation of short and long Bi—$I_{bridging}$ bond distances clearly shows the polar nature of the [BiI_3Cl_2] chain. Interestingly, adjacent chains are related to each other by glide planes, which means that the chain axis corresponds to the *c* polar axis of the crystal (*4mm* point group). The segregation of two kinds of halide ions in such an organic—inorganic hybrid leading to a defined compound is unprecedented.[15] The well-known electron-acceptor viologen entity, which has afforded a great number of charge- or photoinduced charge-transfer salts,[16] is used to interact with neighboring X anions in the solid state through face contacts (X···N^+ or X···$C_{pyridinium}$ σ—π type) and side contacts [X···H(C) π—π^* type].[16] For instance, the equatorial I^- and Br^- in the BiX_5 chains in (MV)[BiX_5] (X = I,[17] Br,[11] respectively) interact with viologen through both face and side contacts. Remarkably, the MV^{2+} dications in (MV)[BiI_3Cl_2], which adopt a twisted conformation, exclusively interact through H···Cl side contacts with the hard halide Cl^- [five H-bonds (<3.0 Å) for each chloride: four H($C_{pyridinium}$)···Cl and one H(CH_3)···Cl] and face contacts with the soft halide I^- (shorter I···"pyridinium plane" distance of 3.745 Å) (Figures 1 and 2). As a result, the Bi(2)I_6 octahedron seems to be encapsulated by eight pyridinium rings while the Bi(1)Cl_4I_2 octahedron and its eight neighboring pyridinium rings adopt a bicalixarene-type form (Figure 2).

Dielectric measurements[18] were performed at different frequencies on a single crystal of **1** between 300 and 400 K with the electric field applied along the [BiI_3Cl_2] chains. Figure 3 shows a weak and monotonic increase in both the dielectric constant (ε') and the losses (tan δ) upon heating. These data show that no dielectric phase transition is present in this temperature range. Nevertheless, a ferroelectric-to-paraelectric transition could occur at higher temperatures. In fact, a sliding of bridging I atoms along the *c* axis, resulting in regular Bi—$I_{bridging}$ bond distances and the presence of a mirror plane containing Bi and equatorial halides, as in the case of the structure of β-(MV)[$BiBr_5$],[11] can be expected. This would lead to a paraelectric phase with $4/mmm$ (D_{4h}) symmetry. Polarization measurements were performed at

dx.doi.org/10.1021/ja206171s |*J. Am. Chem. Soc.* 2011, 133, 14924–14927

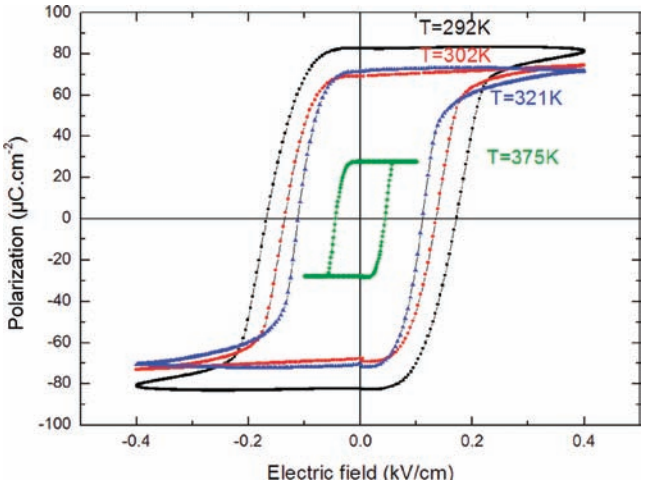

Figure 4. Polarization loops measured on (MV)[BiI_3Cl_2] with the electric field applied along the [BiI_3Cl_2] chains at fixed temperatures of 292, 302, 321, and 375 K with fresh electrical contacts.

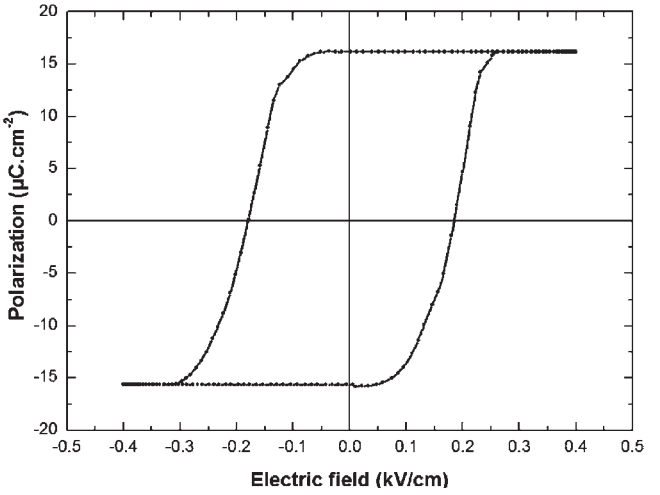

Figure 5. Typical polarization loop observed after five electric field cycles measured on (MV)[BiI_3Cl_2] with the electric field applied along the [BiI_3Cl_2] chains at T = 292 K. A coercive field similar to the one obtained in Figure 4 is observed, but the spontaneous polarization is much smaller.

different temperatures around room temperature[19] on single crystals of **1** with the applied electric field along the [BiI_3Cl_2] chains. As shown in Figure 4, a large polarization loop was observed, with a spontaneous polarization of $P_s \approx 80\ \mu C \cdot cm^{-2}$ and a coercive field of $E_c \approx 0.1-0.2\ kV \cdot cm^{-1}$ at room temperature. This large value of P_s is similar to the highest values reported in the literature in $BiFeO_3$, which is a multiferroic material.[20] As shown in Figure 4, the polarization and coercive field both decreased upon heating. Combined with the absence of any dielectric transition, as shown in Figure 3, these polarization curves indicate the existence of a ferroelectric phase that is stable at temperatures higher than 400 K. However, such large values of P_s were observed only in samples with fresh electrical contacts. After few field sweeps, while the coercive field and the shape of the hysteresis remained nearly unaffected, P_s fell to $10-20\ \mu C \cdot cm^{-2}$ at room temperature, a value which is still high, particularly in the field of hybrid ferroelectrics. Thus, (MV)[BiI_3Cl_2] can be compared for instance to $(EtNH_3)_2[CuCl_4]$[8] and $[CoCl_3(H\text{-}MPPA)]$[1c] [MPPA= (*R*)-2-methylpiperazine], both of which also display clear electrical hysteresis loops with P_s values of $37\ \mu C \cdot cm^{-2}$ (to the best of our knowledge, the highest value ever reported for a hybrid, nevertheless below 247 K) and $6.8\ \mu C \cdot cm^{-2}$ (at room temperature), respectively. Rapid evolution of the polarization loops upon cycling was systematically observed. We believe that this rapid aging effect is related to the strain induced by the large measured polarization, which causes the electrical contacts between the sample and the silver paste used for the contacts to deteriorate quickly.

Indeed, considering for simplicity a simple uniaxial ferroelectric with polarization P and a strain-field component η submitted to an external stress σ, one can perform a Landau expansion of F_s, the free energy for small strains, which gives[21]

$$F_s = \frac{1}{2}K\eta^2 + Q\eta P^2 - \eta\sigma$$

at the lowest order, where K and Q are constants. The first term is related to Hooke's law and corresponds to the elastic energy of the system submitted to the strain. The second term is the lowest-order coupling term between the polarization and the strain, and the last term corresponds to the coupling with the external stress fixed here by the contacts, which are not ferroelectric. Of course, one may add to this Landau expansion the standard term F_P, which is the free energy the in absence of any strain:

$$F_p = \frac{1}{2}a_0(T - T_c)P^2 + \frac{1}{4}bP^4 + \frac{1}{6}cP^6 - EP$$

where a_0 and c are positive constants, b is also a constant, T_c is the Curie temperature, and E is the applied electric field. The minimization of the total free energy, $F = F_P + F_s$, with respect to P and η should then be performed. In particular, the minimization of F with respect to η leads to $\eta = (\sigma - QP^2)/K$. One can consider that no stress is applied before the application of the electric field ($\sigma = 0$). After polarization of the sample with an electric field, a strain proportional to P^2 appears in the sample. Since, P_s appears to be particularly large in our compound, a strong strain develops that may not accommodate the material contact, leading to rapid deterioration of the electrical contacts and a rapid reduction of P_s upon cycling, giving rise to capacitive effects appearing at the contacts and a rapid stabilization of P_s to more standard values of $\sim 15\ \mu C \cdot cm^{-2}$ (Figure 5).

In conclusion, we have presented the synthesis and structural properties of a compound containing mixed-halide chains that exhibits remarkable ferroelectric properties at room temperature. The spontaneous polarization reached values similar to those observed in the best oxide materials. Aging effects reduced this spontaneous polarization to $\sim 15\ \mu C \cdot cm^{-2}$, which is nevertheless a very high value in the field of hybrid ferroelectrics, while the coercive field and the shape of the hysteresis loop ($P_{remanent} \approx P_s$) remained unaffected.

■ ASSOCIATED CONTENT

Supporting Information. Crystallographic data (CIF), X-ray diffraction pattern, thermogravimetric analysis and differential scanning calorimetry curves, and UV−vis spectrum. This material is available free of charge via the Internet at http://pubs.acs.org.

AUTHOR INFORMATION

Corresponding Author

nicolas.mercier@univ-angers.fr; claude.pasquier@u-psud.fr

Present Addresses

[§]Institute of Solid State Physics RAS, Chernogolovka, MD, 142432 Russia.

REFERENCES

(1) (a) Zhang, W.; Ye, H.-Y.; Xiong, R.-G. *Coord. Chem. Rev.* **2009**, *253*, 2980. (b) Zhang, W.; Xiong, R.-G.; Huang, S. D. *J. Am. Chem. Soc.* **2008**, *130*, 10468. (c) Ye, H.-Y.; Fu, D.-W.; Zhang, Y.; Zhang, W.; Xiong, R.-G.; Huang, S. D. *J. Am. Chem. Soc.* **2008**, *131*, 42. (d) Ye, Q.; Song, Y.-M.; Wang, G.-X.; Chen, K.; Fu, D.-W.; Chan, P. W. H.; Zhu, J.-S.; Huang, S. D.; Xiong, R.-G. *J. Am. Chem. Soc.* **2006**, *128*, 6554.

(2) (a) Jain, P.; Ramachandran, V.; Clark, R. J.; Zhou, H. D.; Toby, B. H.; Dalal, N. S.; Kroto, H. W.; Cheetham, A. K. *J. Am. Chem. Soc.* **2009**, *131*, 13625. (b) Jain, P.; Dalal, N. S.; Toby, B. H.; Kroto, H. W.; Cheetham, A. K. *J. Am. Chem. Soc.* **2008**, *130*, 10450. (c) Cui, H.; Wang, Z.; Takahashi, K.; Okano, Y.; Kobayashi, H.; Kobayashi, A. *J. Am. Chem. Soc.* **2006**, *128*, 15074.

(3) (a) Hang, T.; Zhang, W.; Ye, H.-Y.; Xiong, R.-G. *Chem. Soc. Rev.* **2011**, *40*, 3577. (b) Zhang, W.; Chen, L.-Z.; Xiong, R.-G.; Nakaruma, T.; Huang, S. D. *J. Am. Chem. Soc.* **2009**, *131*, 12544. (c) Zhang, W.; Ye, H.-Y.; Cai, H.-L.; Ge, J.-Z.; Xiong, R.-G.; Huang, S. D. *J. Am. Chem. Soc.* **2010**, *132*, 7300.

(4) (a) Jakubas, R.; Krzewska, U.; Bator, G.; Sobczyk, L. *Ferroelectrics* **1988**, *77*, 129. (b) Bujak, M.; Zaleski, J. *J. Solid State Chem.* **2004**, *177*, 3202.

(5) Jakubas, R.; Ciunik, Z.; Bator, G. *Phys. Rev. B* **2003**, *67* No. 024103.

(6) Xu, G.; Li, Y.; Zhu, W.-W.; Wang, G.-J.; Long, X.-F.; Cai, L.-Z.; Wang, M.-S.; Guo, G.-C.; Huang, J.-S.; Bator, G.; Jakubas, R. *J. Mater. Chem.* **2009**, *19*, 2179.

(7) (a) Jakubas, R.; Piecha, A.; Pietraszko, A.; Bator, G. *Phys. Rev. B* **2005**, *72*, No. 104107. (b) Szklarz, P.; Galazka, M.; Zielinski, P.; Bator, G. *Phys. Rev. B* **2006**, *74*, No. 184111.

(8) Kundys, B.; Lappas, A.; Viret, M.; Kapustianyk, V.; Rudyk, V.; Semak, S.; Simon, C.; Bakaimi, I. *Phys. Rev. B* **2010**, *81*, No. 224434.

(9) (a) Horiuchi, S.; Tokunaga, Y.; Giovannetti, G.; Picozzi, S.; Itoh, H.; Shimano, R.; Kumai, R.; Tokura, Y. *Nature* **2010**, *463*, 789. (b) Horiuchi, S.; Tokura, Y. *Nat. Mater.* **2008**, *7*, 357.

(10) (a) Bi, W.; Louvain, N.; Mercier, N.; Luc, J.; Rau, I.; Kajzar, F.; Sahraoui, B. *Adv. Mater.* **2008**, *20*, 1013. (b) Louvain, N.; Mercier, N.; Boucher, F. *Inorg. Chem.* **2009**, *48*, 879.

(11) Bi, W.; Leblanc, N.; Mercier, N.; Auban-Senzier, P.; Pasquier, C. *Chem. Mater.* **2009**, *21*, 4099.

(12) In a 25 mL Teflon bomb were mixed 0.4 mmol of $BiCl_3$, 0.4 mmol of 4,4′-bipyridine, 10 mL of MeOH, 1,7 mL of HCl (36%), and 0.1 mL of HI (57%). The bomb was then sealed in a Parr autoclave and heated in a programmable oven with the following parameters: heating from 25 to 150 °C over 2 h, holding at 150 °C for 13 h, and then cooling to 25°C over 10 h. The in situ formation of MV^{2+} dications, which has been reported previously (see: Hou, J.-J.; Guo, C.-H.; Zhang, X.-M. *Inorg. Chim. Acta* **1996**, *359*, 39) can be explained by the reaction of 4,4′-bipyridine and methyl iodide (also formed in situ by the reaction of methanol and HI). A mixture of dark $(MV)[BiI_3Cl_2]$ crystals and yellow $(MV)_4[Bi_6Cl_{26}]$ crystals[16e] in a ratio of ~9:1 grew and was collected by filtration and washed with methanol. Anal. Calcd for Bi, I, and Cl elements in **1** (atom %): Bi, 16.66; I, 50.00; Cl, 33.33. Found [scanning electron microscopy/energy-dispersive X-ray analysis]: Bi, 16.76; I, 50.04; Cl, 33.21.

(13) X-ray diffraction data for selected single crystals were collected on a Bruker-Nonius Kappa-CDD diffractometer equipped with graphite-monochromatized Mo Kα radiation (λ = 0.71073 Å). Positions and atomic displacement parameters were refined by full-matrix least-squares routines against F^2. All hydrogen atoms were treated with a riding model. Crystal data: $C_{12}H_{14}BiI_3Cl_2N_2$, M = 846.8; tetragonal, *P4nc*; a = 12.5278(10) Å, c = 12.6511(7) Å; V = 1985.5(3) Å^3; Z = 4; T = 293(2) K; $R_1(F)$ = 0.035 [4044 unique reflections in the 3.6−36.0° θ range (R_{int} = 0.044), of which 2334 had $I > 2\sigma(I)$, 99 parameters refined], $wR_2(F^2)$ = 0.084 (all data), GOF = 1.03; racemic twin fraction 0.464(8); max/min residual electron density 1.27/−1.61 e·Å^{-3}.

(14) Brown, D. J. *J. Solid State Chem.* **1974**, *11*, 214.

(15) (a) Kitazawa, N. *Jpn J. Appl. Phys.* **1997**, *36*, 2272. (b) Kitazawa, N. *Mater. Sci. Eng., B* **1997**, *49*, 233. (c) Suzuki, Y.; Kubo, H. *J. Phys. Soc. Jpn.* **1983**, *52*, 1420. (d) Staulo, G.; Bellito, C. *J. Mater. Chem.* **1991**, *1*, 915. (e) Sourisseau, S.; Louvain, N.; Bi, W.; Mercier, N.; Rondeau, D.; Buzaré, J.-Y.; Legein, C. *Inorg. Chem.* **2007**, *46*, 6148.

(16) For recent papers, see: (a) Zhang, Q.; Wu, T.; Bu, X.; Tran, T.; Feng, P. *Chem. Mater.* **2008**, *20*, 4170. (b) Ju, Z.-F.; Yao, Q.-X.; Zhang, J. *Dalton Trans.* **2008**, 355. (c) Xu, G.; Guo, G.; Wang, M.; Zhang, Z.; Chen, W.; Huang, J. *Angew. Chem., Int. Ed.* **2007**, *46*, 3249. (d) Yoshikawa, H.; Nishikiori, S. *Dalton Trans.* **2005**, 3056. (e) Leblanc, N.; Bi, W.; Mercier, N.; Auban-Senzier, P.; Pasquier, C. *Inorg. Chem.* **2010**, *49*, 5824. (f) Tang, Z.; Guloy, A. M. *J. Am. Chem. Soc.* **1999**, *121*, 452.

(17) Chen, Y.; Yang, Z.; Guo, C.-X.; Ni, C.-Y.; Ren, Z.-G.; Li, H.-X.; Lang, J.-P. *Eur. J. Inorg. Chem.* **2010**, 5326.

(18) The dielectric measurements were performed using a Hioki 3522 resistance−inductance−capacitance (RLC) meter with a home-made shielded sample holder.

(19) The polarization loops were obtained using a procedure similar to the one presented by Wegener (see: Wegener, M. *Rev. Sci. Instrum.* **2008**, *79*, No. 106103). The electric field was applied at an ultralow frequency (~10^{-3} Hz) in order to eliminate most capacitive effects. The current through the sample was measured with a Keithley 487 ammeter, which was also used as the electric field source. The time evolution of the current was then numerically integrated in order to get the time evolution of the polarization, which allowed the determination of the $P(E)$ hysteresis loops. The serial resistance and the capacitance of the sample were subtracted before this time integration.

(20) (a) Lebeugle, D.; Colson, D.; Forget, A.; Viret, M. *Appl. Phys. Lett.* **2007**, *91*, No. 022907. (b) Wang, J.; Neaton, J. B.; Zheng, H.; Nagarajan, V.; Ogale, S. B.; Liu, B.; Viehland, D.; Vaithyanathan, V.; Schlom, D. G.; Waghmare, U. V.; Spaldin, N. A.; Rabe, K. M.; Wuttig, M.; Ramesh, R. *Science* **2003**, *299*, 1719.

(21) *Physics of Ferroelectrics: A Modern Perspective*; Rabe, K. M., Ahn, C. H., Triscone, J. M., Eds; Topics in Applied Physics, Vol. 105; Springer: Berlin, 2007.